The onset of fragmentation in binary liquid drop collisions

C. Planchette[1], E. Lorenceau[2], G. Brenn[3*]
[1]Research Center Pharmaceutical Engineering, Graz, Austria
[2]Laboratoire Navier, UMR 8205 - CNRS, Université Paris-Est, France
[3]Institute of Fluid Mechanics and Heat Transfer, Graz University of Technology, Austria
brenn@fluidmech.tu-graz.ac.at and carole.planchette@tugraz.at

Abstract

Binary collisions of drops of immiscible liquids are investigated experimentally at well defined conditions of impact. In the experiments we vary all relevant properties of an aqueous and an oil phase, the impact parameter, the drop size and the relative velocity. The drops observed after the collisions exhibit three main phenomena: full encapsulation, head-on fragmentation, and off-centre fragmentation. The regimes characterised by these phenomena replace the ones observed in binary collisions of drops of the same liquid: coalescence, reflexive separation, and stretching separation. Our aim is a universal description of the fragmentation thresholds of head-on collisions. Based on the capillary instability and an energy balance, we establish a scaling law for the evolution of the threshold impact velocity with the properties of the liquids and the droplet size. Our work yields new insight into binary collisions of drops and proposes a perspective to develop a more general description with implications for binary collisions of drops of a single liquid as well.

Introduction

First investigations of binary water drop collisions were triggered by meteorological interest for their importance in rainfall [1]. Technical interest in spray combustion and spray drying motivated investigations on the stability behaviour of colliding drops and the outcome from the drop collisions for liquids other than water also [2]-[5]. In all these studies, the colliding drops consisted of the same liquid. More recently, investigations on collisions of drops consisting of different, in part immiscible, liquids began [6]-[8]. The fields of technical applications of this kind of drop collisions may range from combustion in engines to production processes in some life sciences, such as the coating of a liquid core by another, immiscible liquid.

For colliding drops of the same liquid and size, the collision outcome is determined by the drop diameter D and relative velocity U, the impact parameter x of the collision (figure 1 left), and by the density ρ, dynamic viscosity μ, and surface tension σ of the droplet liquid against the ambient air. The outcome of the collision may therefore be represented non-dimensionally by the non-dimensional impact parameter $X = x/D$ and the Weber and Ohnesorge numbers, $\rho U^2 D/\sigma$ and $\mu/\sqrt{\sigma D \rho}$, respectively. This set of numbers, preferred in the state-of-art literature, however, is not the only possible one. Alternatively one can represent the evolution of the Reynolds number $\rho U D/\mu$ with the Ohnesorge number, for example.

In the above case, the outcome from a collision with a given Ohnesorge number may be represented in the form of a nomogram ($X,\ We$). The four regimes coalescence, bouncing, stretching separation, and reflexive separation may be identified in the ($X,\ We$) nomogram for the head-on ($X \approx 0$) and the off-centre ($X \neq 0$) cases, as shown in figure 1 right [4]. In their study of collisions of equal-sized drops of the immiscible liquids diesel oil and water, Chen & Chen found the same regimes of outcomes of the collisions, characterized by the non-dimensional impact parameter X and the Weber number We based on the properties of the Diesel oil [7]. The shapes of the regimes in the ($X,\ We$) nomogram are very similar to the ones found, e.g., in [4] in single-fluid drop collisions. Additionally, however, Chen & Chen found a mechanism termed "single-reflex" separation, where only the water drop is reflected from the plane of impact, while the Diesel oil drop flows around the surface of the water drop. In our work [8] we found one further mechanism of immiscible liquid drop collisions which we termed "crossing separation". This mechanism consists in a motion of the oil phase on the aqueous drop to the side opposite from the impact, from where a drop of pure oil may pinch off. We discuss these mechanisms in detail below.

Compared to the studies of binary drop collisions known from the literature, the introduction of two different immiscible liquids appears to be a problem of higher degree of complexity at the first glance. It has, however, proven to be a powerful way to analyse the different phenomena in the entire process. In this paper we use this configuration to test the influence of the relevant parameters and develop satisfactory physical interpretations of the fragmentation threshold for head-on collisions.

*Corresponding author: brenn@fluidmech.tu-graz.ac.at

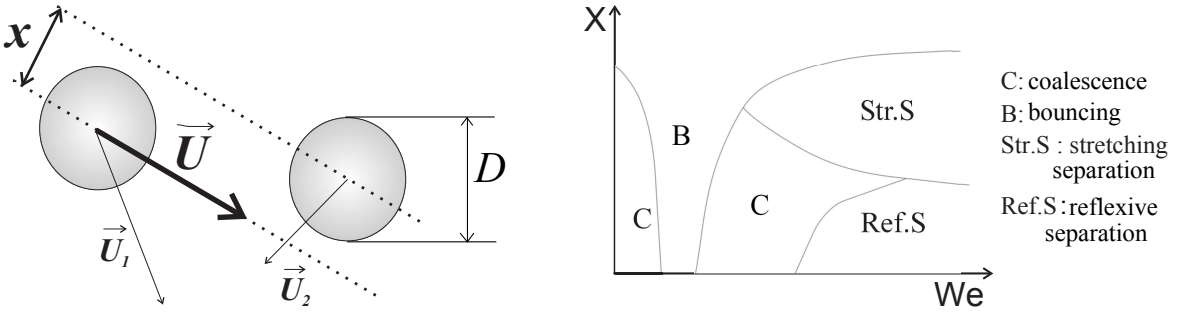

Figure 1. Left: Geometric and kinetic parameters of binary drop collisions. Right: Sketch of the stability nomogram for binary drop collisions with a single liquid for a given Ohnesorge number, where $We = \rho U^2 D/\sigma$ (adapted from [4]).

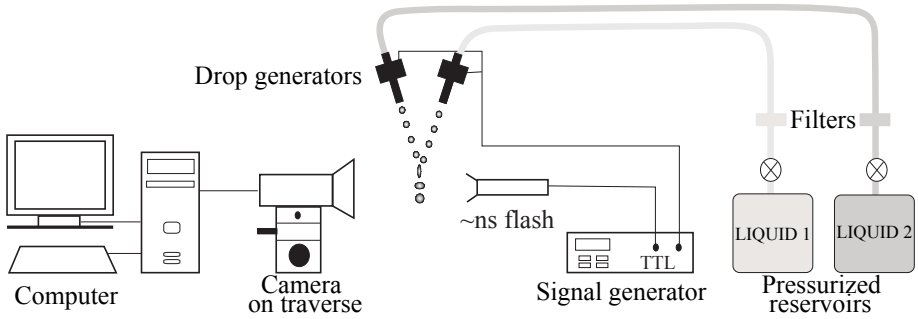

Figure 2. Experimental set-up with two droplet generators connected to two immiscible liquid reservoirs. The generator positions can be adjusted with micro-control traverses. The ultrafast flash illuminates the colliding drops. Images are recorded by the camera.

We first present the setup and materials used for the experimental part of the study, describe the main regimes of phenomena observed, and compare them to the ones for binary collisions of drops of the same liquid. The fragmentation threshold for head-on collisions is then discussed. We then present a quantitative analysis for the threshold velocity of head-on collisions. The experimental results and their theoretical interpretation are validated for a large range of parameters. The paper ends with the conclusions.

Experimental set-up and materials

Experimental set-up and measuring techniques

In order to produce well defined collisions of two drops of immiscible liquids we use two droplet generators connected to two pressurized tanks, each of them containing one of the two immiscible liquids (figure 2). The droplet generators produce reproducible and monodisperse drop streams by controlled jet break-up by the Rayleigh-Plateau instability [9]. The nozzles may produce droplets of diameters ranging from 150 μm to 350 μm with a typical frequency of 10 kHz. For accurately adjusting the trajectories of the drops, the generators are fixed on translation and rotation stages. The accuracy of their displacements is estimated to be of the order of ± 2 μm and ± 2 °, respectively. The colliding droplets are illuminated by flashes of some nanoseconds duration. Images are recorded by a high-resolution PCO video camera Sensicam.

With the frequency of drop formation known, we deduce from these pictures size and relative velocity of the drops, as well as the impact parameter. The drop size D is obtained from the area A of the projection of the drop on the CCD array of the camera, using the equation $D = 2\sqrt{A/\pi}$. The resolution of our imaging system is 5 μm/pixel, which leads to an accuracy of the drop diameter measurement of ± 2 μm. The relative velocity and impact parameter are deduced from the relative positions of the drop centres of mass by vector calculation. Following this procedure, the accuracy is estimated to be of 1%. Since the formation of the drop streams is highly reproducible, pictures of several drop pairs generated at successive instants represent the time evolution of a given single pair of drops. In all of the pictures presented later in this paper, the elapsed time between two successive pairs of drops is 100 μs, and the drop size is 200 μm. The dark liquid is a dyed aqueous solution of glycerol, while the transparent drops consist of oils.

Aqueous solutions % mass	Density kg/m^3	Dynamic viscosity mPa·s	Surface tension mN/m	Interfacial tension mN/m
Glycerol 20%	1047.9	1.76	70.7	37.7[1]
Glycerol 30%	1072.9	2.50	70.3	36.7[1]
Glycerol 40%	1098.8	3.72	69.5	34.9[1]
Glycerol 50%	1126.0	6.00	68.6	34.8[1]
Glycerol 50%	1126.0	6.00	68.6	34.3[2]
Glycerol 55%	1139.0	7.90	68.1	33.8[1]
Glycerol 60%	1153.8	10.8	68	

Oils	Density kg/m^3	Dynamic viscosity mPa·s	Surface tension mN/m	Interfacial tension mN/m
SOM3	892.2	2.79*	19.5*	34.9[3]
SOM5	913.4	4.57*	19.5	-
SOM5+10	925.3	6.6	19.8	-
SOM10	937.2	9.37*	20.1	-
SOM10+20	944.5	14.28	20.3	-
SOM20	951.8	19.0*	20.7	-
PERFLUO	1934.9	5.5*	17.8	36.5[3]

Table 1. Left: Properties of the aqueous glycerol solutions at 20°C. Glycerol concentrations are given in mass percent. Interfacial tensions correspond (1) to SO M3, (2) to SO M5. Right: Properties of the oils at 20°C.(+) Mixtures of two oils. (*) Values given by the data sheet of our supplier Carl Roth. (3) Interfacial tensions are given for contact with a glycerol solution at 50%.

Immiscible liquids

With the aim to achieve full encapsulation of one liquid by another one, we selected immiscible liquids with total wetting properties. The encapsulated phase is an aqueous solution of glycerol at varying concentration. The viscosity of these solutions can be tuned from less than 2 $mPa \cdot s$ to more than 10 $mPa \cdot s$ without noticeable changes of the other parameters (table 1 left). The encapsulating phase is a silicon oil with a viscosity between 3 $mPa \cdot s$ and 20 $mPa \cdot s$. Perfluorodecalin is also used, which allows us to measure the effect of a density change (table 1 right).

In this paper, the aqueous solutions are denoted by the subscript *water*, and the oils by the subscript *oil*. For all combinations we checked the total wettability of the aqueous solutions by the oils. Surface and interfacial tensions, measured with the pendant drop method (tensiometer LAUDA TVT-1) and listed in tables 1 left and right, show very little variation. The surface energy contribution is therefore always of the same order and is not going to be deeply addressed in the theoretical part of our study.

Main regimes for head-on collisions

As for the collisions of drops of the same liquid, nomograms can be built to qualitatively show regimes characterized by different phenomena after the collisions. In contrast to the classical collisions, we decided not to use the Weber number but the relative velocity U of the drops, since the Weber number definition is not clear any more as two surface tensions and one interfacial tension coexist. The following regimes are observed for head-on collisions:

- *Full encapsulation* for moderate impact parameters and moderate relative velocities. The oil droplet spreads on the aqueous one and fully remains around it, forming a liquid shell. Such an encapsulated drop is thus composed of an aqueous core coated by an oil film. The excess of energy resulting from the collision and leading to a strong distortion of the drops is dissipated, and the encapsulated drop finally assumes the expected spherical shape (figure 3). If the liquids were miscible, the regime of coalescence would replace the encapsulation.

- For higher relative velocity and small impact parameter close to zero, *fragmentation for head-on collisions* is observed. The collision complex generated by the impact relaxes from a disk-like shape (a thin lamella with a rim) to a cylinder. Fragmentation is brought about by break-up of the cylinder and generates two main drops. Overall we see three typical cases: the so-called "crossing separation" [8] produces a single encapsulated drop plus a smaller pure oil drop ejected from the side opposite to the side of the original drop arrival; "single-reflex separation" [7, 8] where the aqueous drop is split up, resulting in two encapsulated drops, and finally "quasi-reflexive separation" generating a single encapsulated drop plus a much smaller pure oil droplet located on the side of the original oil droplet approach. These three subclasses representing "fragmentation for head-on collisions" are shown in the pictures of figure 4. For miscible liquids we see the regime of reflexive separation instead.

Figure 3. Full encapsulation of a 50 % glycerol solution drop by SO M20. The relative velocity of the drops at the impact is 3.88 m/s.

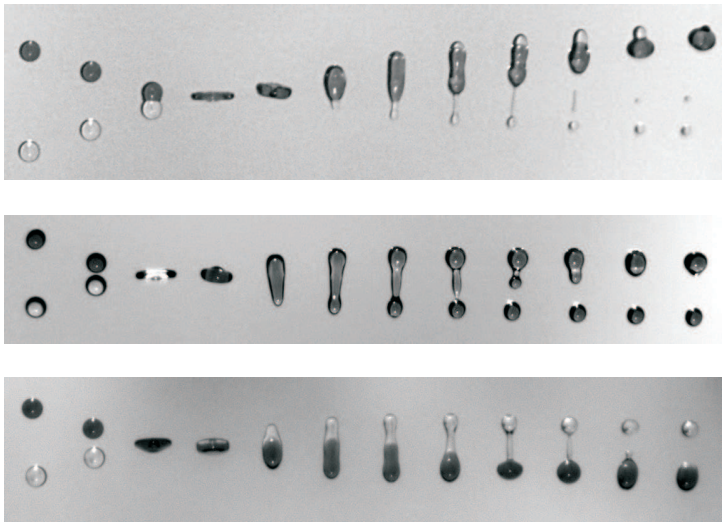

Figure 4. Examples of head-on fragmentation showing the three typical liquid distributions. From top to bottom,"quasi-reflexive separation" (G50 and perfluorodecaline, U=3.95 m/s), "single-reflex separation" (G20 and SO M10, U=4.32 m/s), and "crossing separation" (G50 and SO M5, U=3.97 m/s).

For head-on collisions, the full encapsulation and fragmentation regimes are defined by the threshold velocity U_c. This velocity is experimentally obtained as the mean of the highest and lowest velocities leading to full encapsulation and fragmentation, respectively. The typical uncertainty of U_c is less than $\pm$ 0.1 m/s.

Looking at the various outcomes from the collisions, the problem of understanding and describing the transitions between the regimes naturally arises. For head-on collisions, the question can be formulated as "how large is the threshold velocity between full encapsulation and fragmentation?" We provide an answer in the form of a scaling law representing the experimental data over wide ranges of the experimental parameters.

Head-on collisions: onset of fragmentation

In order to develop an analytical expression for the threshold velocity U_c between full encapsulation and fragmentation for head-on collisions, we first develop a fragmentation criterion. This criterion emerging from surface energy considerations and validated by experimental observation is presented in the following subsection. We then propose to divide the collision into two main processes, allowing us to relate our fragmentation criterion to the initial state of the drops. The first phase corresponds to the deformation of the drops by the impact. It lasts until the collision complex has reached its maximum extension and the shape of a flat disk. Because of the analogy between a drop and a spring [10], we will refer to this phase as the "compression phase", noting nonetheless that the liquids do not undergo any compression themselves. A second phase follows, where this liquid "disk" relaxes, forming a liquid cylinder. The associated energy losses are discussed in the related sections. The theoretical expression for U_c is finally compared to the experimental results.

Fragmentation criterion

The fragmentation of the liquid cylinder formed after the collision, producing two drops of almost equal size, suggests a mechanism similar to a static cylinder break-up, known as the Rayleigh instability. For length-to-diameter (aspect) ratios above π, a liquid cylinder breaks up into equal-sized drops, minimizing the total surface energy. This mechanism of fragmentation has already been considered in [2] for binary collisions of water drops

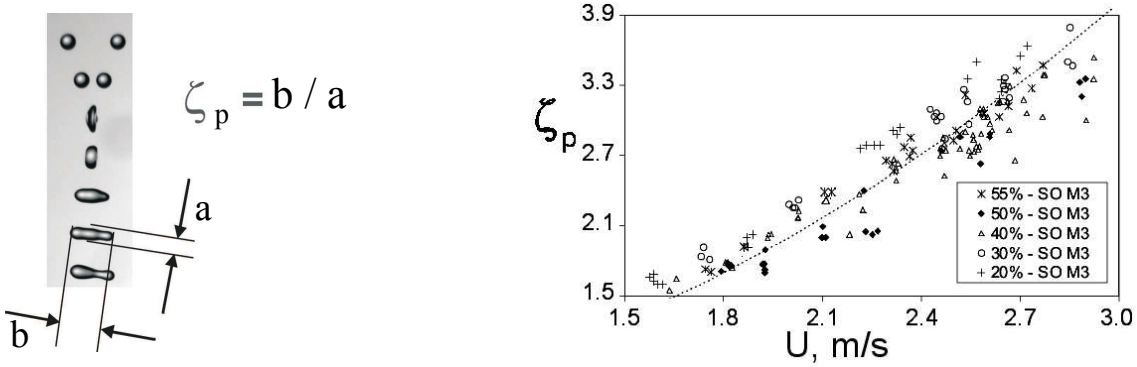

Figure 5. Left: Definition of ζ_p, the aspect ratio of the liquid cylinder resulting from the collision. Right: Evolution of ζ_p with the relative velocity of the drops at impact for different glycerol concentrations. The viscosity ranges from 1.8 $mPa \cdot s$ to 7.9 $mPa \cdot s$. The oil was SO M3 in all cases. All data points are distributed along a single curve. The fit curve corresponds to $\zeta_p = 0.4 + 0.4U^2$.

undergoing reflexive separation. To validate the fragmentation criterion, we measure the aspect ratios $\zeta_p = b/a$ of the liquid cylinders on the images. The aspect ratio ζ_p is defined in figure 5 left. The values are collected for several glycerol concentrations, and the relative velocity of the drops is varied including both regimes of encapsulation and fragmentation. All these data are shown in figure 5 right. Despite the glycerol solution viscosity variation from below 2 $mPa \cdot s$ to almost 8 $mPa \cdot s$, all data points are distributed along a single curve. We then determine the critical aspect ratio $\zeta_{p,crit}$ for the transition from full encapsulation to fragmentation. The critical aspect ratio is found to be independent of the aqueous phase viscosity (data not presented here), and the value of the order of 3 measured is very close to the Rayleigh value of π. This result is surprising: it suggests that there is no influence of the finite size of the cylinder, nor of the internal flow of the two liquids on the fragmentation mechanism. Yet, it is known from the literature that the fragmentation of a stretched liquid cylinder is totally different from the classical break-up problem of Rayleigh Plateau [11]. In our case the break-up always occurs slightly before the maximum extension state of the liquid cylinder. Actually, the images of figure 4 show that the liquid cylinder breaks up about 600 μs to 700 μs after the collision (6th or 7th position counted from the instant of first contact of the drops), which corresponds to the expected oscillation period for the base mode of the encapsulated drop with twice the volume of the colliding drops: $T = (\pi/4)\sqrt{\rho_{oil} 2D^3/\sigma_{oil}} \approx 700\ \mu s$. Thus, the internal flows within the liquid cylinder enhance the break-up, rather than preventing it.

In the next sections we focus on two successive phases of the collision with the aim to relate the fragmentation criterion established above to the initial kinetic energy using the intermediate complex state of maximum extension.

Compression

We first estimate the energy loss of the "compression" phase, which turns the two drops into a thin lamella bounded by a rim (figure 6). This structure looks like a disk in a side view (e.g., figure 4). Knowing the initial kinetic and surface energies, we can deduce the energy loss in this "compression" period. An accurate observation of the drops at the very early stage of the collision shows that the encapsulation of the aqueous core by the oil film is complete before the complex reaches its maximum extension. This suggests to estimate the surface energy of the disk ($E_{\sigma\ disk}$) as:

$$E_{\sigma\ disk} = \left(\sigma_{oil} + \sigma_{water/oil}\right) \pi D_{max}^2 \tag{1}$$

The temporal and spatial resolutions of our images allow us to measure the maximum diameter of the complex, which we estimated for several pairs of liquids and a wide range of velocities, independent from the regime observed. Typical results are presented in the figure 7 left. We use these experimental results in combination with the following energy balance to deduce the energy loss E in this first period:

$$E = E_k + E_{\sigma\ ini} - E_{\sigma\ disk} \tag{2}$$

In this balance, E_k and $E_{\sigma\ ini}$ are the initial kinetic and the initial surface energies, respectively. Obviously, $E_k = \pi\left(\rho_{water} + \rho_{oil}\right) D^3 U^2/48$ and $E_{\sigma\ ini} = \pi D^2\left(\sigma_{water} + \sigma_{oil}\right)$.

As seen in the figure 7 right, this loss is almost independent of the oil viscosity, since it increases only by a few percent as the viscosity is increased by a factor of 3. We also observe that the energetic loss increases

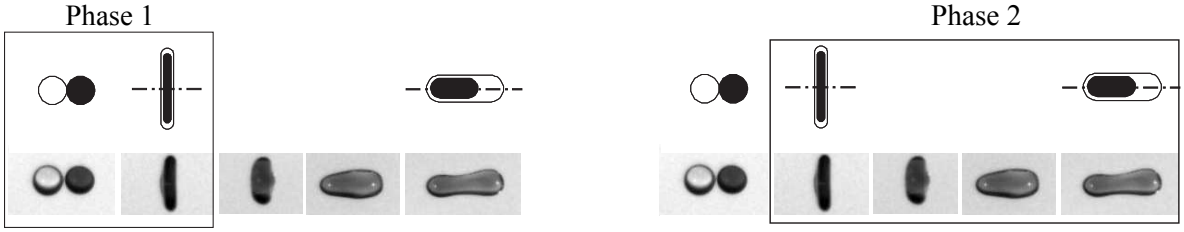

Figure 6. Structure of the collision process in two phases. Phase 1 (framed left): from the first contact until the maximum extension of the complex, followed by phase 2 (framed right), where the disk relaxes into a cylinder. The time between two successive pictures is 100 μs. The distribution of the two liquids in the case depicted here is not representative of all cases observed.

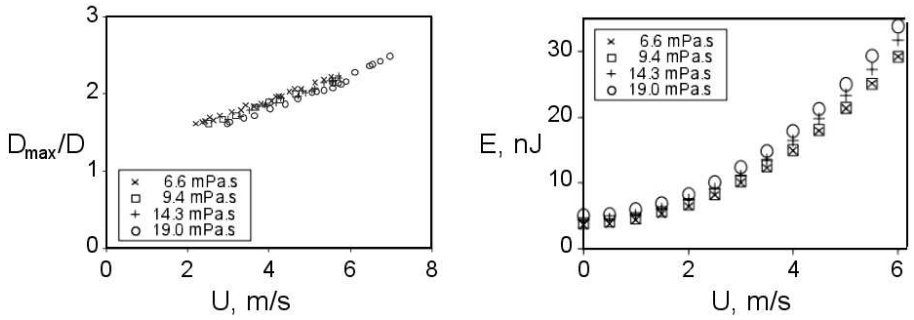

Figure 7. Left: evolution of the maximum extension of the disk with the relative drop velocity U for different oils. The oil viscosity ranges from 6.6mPa·s to 19 mPa·s, the glycerol concentration is constant (50 %). Right: evolution of the energy loss E between the initial state and the disk at its maximum extension for the same combinations of liquids as on the left. E is found to be quasi-inertial, independent from the oil viscosity.

with the velocity squared. This suggests an inertial energetic loss, and normalizing this inertial part by the initial kinetic energy of the drops leads to the result that 94 % of the initial kinetic energy is lost. It is interesting to note that similar results have also been observed for binary collisions of drops of the same liquid by [3], and for the impact of drops on a solid surface by, e.g., [12]. In those symmetric impact situations, the flow is highly dissipative: while the energy conservation would lead to $D_{max}/D_{oil} \sim \sqrt{We/6}$, the momentum conservation yields $D_{max}/D_{oil} \sim 0.12\sqrt{We}$. Thus, the inertial loss measured when the drops reach the maximum extension can reach $1-6\cdot 0.12^2 = 0.91$, which corresponds to 91 % of the initial kinetic energy, in the same order of what is observed for immiscible liquids. This inertial loss can be interpreted as a consequence of the rim formation, where all the incoming kinetic drop energy absorbed is basically dissipated.

As a consequence, we will consider in the rest of this paper that only 6% of the initial kinetic energy remains for the second phase of the collision. Having already have a fragmentation criterion, we now aim at describing the second (relaxation) phase.

Relaxation of the disk

In the second phase of the collision, the disk relaxes into a cylinder (figure 6 right). As mentioned, we can use an analogy between a drop and a spring [10]. More precisely, during its "compression phase", the kinetic energy of the drop is partially transformed into surface energy. This excess of energy is then dissipated by the drop oscillation in the relaxation phase. This second phase can thus be treated as the relaxation of a compressed spring oscillating around its equilibrium position. For our drop collisions, oscillations are strongly damped by the liquid viscosity, leading to an aperiodic relaxation. We now aim to relate the complex at its maximum extension to the fragmentation criterion in order to establish a relation between the initial state of the drops and the threshold velocity U_c. As the encapsulation is complete when the disk reaches its maximum extension, we can consider that this relaxation phase corresponds to an aperiodic oscillation of an encapsulated drop. Excluding the contributions from surface energies, the energy balance of this second phase is reduced to

$$E_k - E = E_\mu \tag{3}$$

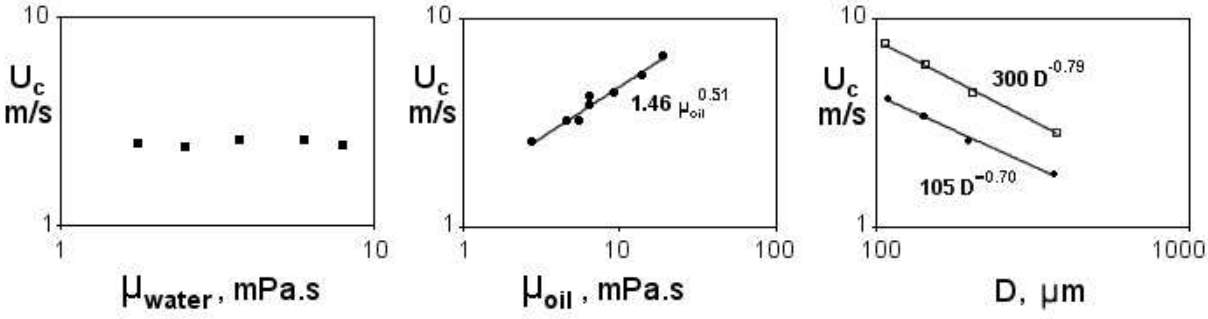

Figure 8. Evolution of the measured threshold velocity with (from left to right) the aqueous solution viscosity (μ_{oil} = 2.79 mPa·s), the oil viscosity (μ_{water} = 6 mPa·s), and the drop diameter (aqueous phase G50, oil phase - upper line SO M10, lower line SO M3). The powers μ_{water}^{0}, $\mu_{oil}^{1/2}$, and $D^{-3/4}$ of the scaling law (7) are in very good agreement with the experimental data.

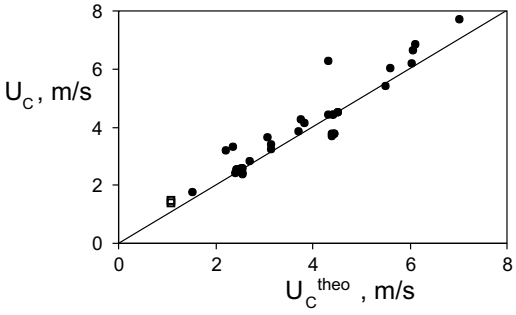

Figure 9. Comparison of the experimental threshold velocities with the theoretical values given by equation (7). All results are shown, including all liquids of tables 1 left and right and the various drop diameters of figure 8 between 150 μm and 360 μm. The data corresponding to collisions of diesel oil and water drops of 750 μm diameter, extracted from [7], is also plotted (open squares). The straight line indicates $U_c = U_c{}^{theo}$

where E_μ is the viscous loss during the relaxation of the disk.

For estimating E_μ after the maximum extension phase we assume that the viscous loss is confined to the oil film, where the largest velocities are reached. This hypothesis is in good agreement with the experimental result that the threshold velocity does not depend on the encapsulated phase viscosity. In the oil film, the velocity gradients occur on a typical thickness $h \approx D$, thus yielding the expression

$$E_\mu \approx \mu_{oil} \left(\frac{V_{relax}}{h} \right)^2 \pi D^3 \frac{D}{V_{relax}} \approx \mu_{oil} \frac{V_{relax}}{D} \pi D^3 \tag{4}$$

for the viscous loss during the second phase of the impact, where V_{relax} is the relaxation velocity after the collision. It can be evaluated as proposed in [13] as $V_{relax} \approx L/\tau_i$, where $\tau_i \approx (D^3 \rho_{oil}/\sigma_{oil})^{1/2}$ corresponds to the capillary oscillation period of an inviscid droplet and L is the maximum extension of the drop. As a result, the energy dissipated by viscosity comes out as

$$E_\mu = \mu_{oil} \sqrt{\frac{\sigma_{oil}}{\rho_{oil} D^3}} \pi D^3 \frac{L}{D} \tag{5}$$

The obtained viscous dissipation is independent of the impact velocity U. This remarkable feature can be understood in the framework developed by [10, 14] for the impact of a single drop on a solid surface: The rebound is globally considered as an oscillation. In this framework, the drop is a spring of stiffness σ and mass ρD^3, which oscillates with a period in the order of $(D^3 \rho/\sigma)^{1/2}$. We then identify the ratio L/D as the aspect ratio of the cylinder ζ_p and balance the kinetic energy left after the expansion of the disk by this viscous loss. This yields

$$\mu_{oil} \sqrt{\frac{\sigma_{oil}}{\rho_{oil} D^3}} \pi D^3 \zeta_p \approx E_k - E = \frac{0.06\pi}{48} \left(\rho_{oil} + \rho_{water} \right) D^3 U^2 \tag{6}$$

We make use of the fragmentation criterion to finally obtain the threshold velocity ${U_c}^{theo}$. Indeed, we consider that the cylinder breaks up for $\zeta_p = \pi$. This leads to

$$ {U_c}^{theo} = \sqrt{\frac{48\pi}{0.06}\frac{\mu_{oil}}{\rho_{oil}+\rho_{water}}\sqrt{\frac{\sigma_{oil}}{\rho_{oil}D^3}}} \;; \qquad \text{i.e.,} \qquad Re \propto \sqrt{\frac{\rho_{oil}+\rho_{water}}{\rho_{oil}}} Oh_{oil}^{-1/2} \tag{7} $$

where $Re = U_c^{theo}(\rho_{oil}+\rho_{water})D/2\mu_{oil}$ and $Oh_{oil} = \mu_{oil}/\sqrt{\sigma_{oil}D\rho_{oil}}$. The scaling law thus established corresponds to a variation of the threshold velocity with μ_{water}^0, $\mu_{oil}^{1/2}$, and $D^{-3/4}$. These three powers obtained theoretically are very well confirmed by the experimental results shown in figure 8. Our data, plus the results by Chen & Chen, are represented in figure 9 together with the theoretical evaluation of ${U_c}^{theo}$. This includes a wide range of combinations of liquids (glycerol solutions with viscosities ranging from $1.8mPa\cdot s$ to $10.8mPa\cdot s$, silicon oils with viscosities varying from $2.8mPa\cdot s$ to $19mPa\cdot s$, plus one fluorinated oil with the double density) and drop diameters from $150\mu m$ to $350\mu m$. We may emphasize that the agreement between these experimental results and the theoretical expression is very good: the slope between the experimental data and the theoretical prediction deduced from our analysis captures the fragmentation mechanism.

Conclusions

We investigated the onset of fragmentation after binary collisions of drops of immiscible liquids. The experimental results obtained for a wide range of liquids are presented and tested against theoretical and empirical models.

For the head-on configuration, the collision process is found to be similar to a succession of compression and relaxation of the drops. The fragmentation criterion can be reduced to the well known Rayleigh criterion for capillary instability. As for collisions of drops of the same liquid, the first period of the collision, during which the drops are distorted to form a lamella surrounded by a rim, generates inertial energy losses. We interpret this phenomenon as the consequence of the formation of flow fields inside the drops. The losses are found to be more important in the case of immiscible liquids than for drops of the same liquid, which is coherent with a difference in the respective flow fields. In contrast to binary collisions of drops of the same liquid, for the presently investigated liquids, the viscous dissipation of the second phase of the process is confined to the oil film and can therefore be easily expressed using the analogy with the relaxation of an encapsulated drop. For drops of the same liquid, literature data show two regimes depending on the importance of the viscous as compared to the oscillation time scales. This transition could also exist for immiscible liquids in viscosity ranges not studied in our experiments.

Acknowledgements

The authors gratefully acknowledge Michèle Adler for her support as well as several fundings: the Hubert Curien Program AMADEUS 2009 from the French Ministry of Foreign Affairs and the Austrian ÖAD and the European COST Action P21 - Physics of Droplets. Financial support from the Steiermärkische Landesregierung for C.P. is gratefully acknowledged. We wish to thank the institute CVTUT of Graz University of Technology for support in the measurements of interfacial tensions.

References

[1] Brazier-Smith, P. R., Jennings, S. G., Latham, J., *Proceedings of the Royal Society London A* 326:393-408 (1972)
[2] Ashgriz, N., Poo, J. Y., *Journal of Fluid Mechanics* 221:183-204 (1990)
[3] Jiang, Y. J., Umemura, A., Law, C. ,K., *Journal of Fluid Mechanics* 234:171-190 (1992)
[4] Qian, J., Law, C.K., *Journal of Fluid Mechanics* 331:59-80 (1997)
[5] Brenn, G., Valkovska, D., Danov, K. D., *Physics of Fluids* 13:2463-2477 (2001)
[6] Gao, T.-C., Chen, R.-H. & Lin, T.-H. *Experiments in Fluids* 38:731-738 (2005)
[7] Chen, R.-H., Chen, C.-T., *Experiments in Fluids* 41:453-461 (2006)
[8] Planchette, C., Lorenceau, E., Brenn, G., *Colloids and Surfaces A* 365:89-94 (2010)
[9] Brenn, G., Durst, F., Tropea, C., *Particle and Particle Systems Characterization* 13:179-185 (1996)
[10] Richard, D., Clanet, C., Quéré, D., *Nature* 417:811 (2002)
[11] Rayleigh, Lord, *Proceedings of the Royal Society London A* 29:71-97 (1879)
[12] Eggers, J., Fontelos, M. A., Josserand, C., Zaleski, S., *Physics of Fluids* 22:062101 (2010)
[13] Bartolo, D., Josserand, C., Bonn, D., *Journal of Fluid Mechanics* 545:329-338 (2005)
[14] Biance, A.L., Chevy, F., Clanet, C., Lagubeau, G., Quéré, D., *Journal of Fluid Mechanics* 554:47-66 (2006)